Fire Safety Journal 148 (2024) 104226

Contents lists available at ScienceDirect

Fire Safety Journal

journal homepage: www.elsevier.com/locate/firesaf

Smoldering ignition and transition to flaming in wooden mulch beds exposed to firebrands under wind

Shaorun Lin [a,*], Chengze Li [a], Mackenzie Conkling [a], Xinyan Huang [b], Stephen L. Quarles [c], Michael J. Gollner [a,**]

[a] Department of Mechanical Engineering, University of California, Berkeley, CA, United States
[b] Research Center for Smart Urban Resilience and Firefighting, Department of Building Environment and Energy Engineering, The Hong Kong Polytechnic University, Kowloon, Hong Kong
[c] University of California Cooperative Extension (Emeritus), Mill Valley, CA, United States

ARTICLE INFO

Keywords:
Wildland-urban interface
Particle size
Firebrand
Smoldering-to-flaming transition
Ember

ABSTRACT

Spotting ignition by firebrands is a significant fire spread pathway at the wildland-urban interface (WUI), where mulch products are commonly used as landscaping materials. Mulch is typically organic in nature, thus it may be easily ignited into a smoldering mode by firebrands and subsequently transition to flaming, leading to direct flame contact and radiant heat exposure to siding materials of adjacent structures. This work quantified the thresholds of smoldering ignition of four common types of commercially available mulch (black mulch (BM), forest floor (FF), redwood (RW), and fir bark (FB)) exposed to heating by smoldering firebrand piles, and their propensity for smoldering-to-flaming transition under external winds (up to 1.4 m/s). We found that there was a minimum mass of firebrand pile to achieve smoldering ignition of mulch (e.g., ~0.1 g for FF). Beyond this minimum mass, the required wind speed to trigger smoldering ignition generally decreased as the mass of the firebrand pile increased, agreeing well with theoretical analysis. After smoldering ignition, smoldering-to-flaming transition could be observed when the wind speed exceeded a critical value (e.g., ~1 m/s for FF), which was not affected by the initial spotting process. To achieve smoldering-to-flaming transition, the glowing mulch had to reach a critical temperature of around 850 °C. Mulch samples with larger particle sizes were more likely to smolder and transition to flaming, due to increased oxygen supply through larger inter-particle pores and channels and better firebrand accumulation due to a more crevice-like geometry on the fuel surface. This work advances the fundamental understanding of the ignition and burning behavior of landscaping mulches, and thus contributes to the prevention of extreme WUI fire events.

Nomenclature

Symbols		Greek Symbols	
c	Specific heat capacity (J/(kg-K))	α	ratio of heat transferred from the firebrand pile to the mulch sample (−)
D	diameter (m)	γ	stoichiometric factor (−)
E	energy (J)	ρ	bulk density (kg/m^3)
E''	Energy per unit area (J/m^2)	ρ_b	bulk density (kg/m^3)
ΔH	heat of reaction (MJ/kg)	ρ_s	solid density (kg/m^3)
m	mass (g)		
$\dot{m}''$	mass flux (g/m^2·s)	Subscripts	
n	number (−)	a	air
$\dot{q}''$	heat flux (kW/m^2)	$cond$	conduction
r	radius (m)	$conv$	convection
T	temperature (°C)	fb	firebrand
t	time (s)	min	minimum
v	wind speed (m/s)	ox	oxygen or oxidizer
Y	mass fraction (−)	r	radiative
		sm	smoldering
		T	thermal

(continued on next column)

(continued)

* Corresponding author. 60 Hesse Hall, Berkeley, CA 94709, United States.
** Corresponding author. 6105A Etcheverry Hall, University of California, Berkeley, CA, 94720, United States.
E-mail addresses: shaorun.lin@berkeley.edu (S. Lin), mgollner@berkeley.edu (M.J. Gollner).

https://doi.org/10.1016/j.firesaf.2024.104226
Received 13 March 2024; Received in revised form 3 June 2024; Accepted 15 July 2024
Available online 17 July 2024

1. Introduction

Climate change, population growth, and evolving practices in the development and management of natural lands have increased the risk of high-intensity wildfires. Fires at the wildland-urban interface (WUI), where natural lands adjacent to human development, are particularly destructive as they often directly impact people and communities [1]. Spotting ignition by smoldering firebrands is a critical fire spread pathway that is prevalent at the WUI [2,3]. These combustible fragments (i.e., firebrands) are primarily generated from burning wildland fuels and wood-based structures when they lose their structural integrity and break into smaller pieces due to the drag forces from surrounding airflow [4,5]. Subsequently, they can be lofted long distances by external winds or buoyancy through fire-induced plumes, igniting structures or vegetative fuels far ahead of the fire front (up to 30–40 km) [2,6]. Recent data suggests that at least 50 % of ignitions during WUI fires, and potentially even more, can be attributed to firebrands [7]. A notable example of the significance of firebrand processes is the 2018 Camp Fire in Northern California, leading to 85 causalities, over 18,800 structures destroyed, and 153,000 ha burnt, with long-range firebrand spotting having contributed to the extensive destruction which primarily occurred within the first few hours [8,9].

At the WUI, mulch products are commonly used as landscaping materials around residential structures and in community parks for a variety of reasons (e.g., improving the fertility of the soil and visual appeal of the area) [10,11]. Typically, though not exclusively organic in nature, mulch can be easily ignited by firebrands, either in smoldering (may subsequently transition to flaming) or direct flaming ignition modes [12]. Without proper clearance around the base of a structure, burning mulch can pose a significant ignition hazard to the adjacent buildings as it can lead to direct flame contact and radiant heat exposure to siding materials, windows, or other features along exterior walls [6]. On a community level, maintaining adequate space between mulch and structures is crucial in mitigating fire risk, and several design recommendations have been proposed to prevent this issue [6,13,14]. However, more fundamental studies are still required to improve our understanding of mulch burning and enrich the prevention and mitigation strategies.

Understanding the spotting ignition of mulch is essential for evaluating the initiation and growth of subsequent fire events. Ignition of mulch is expected to differ from ignition of solid recipient fuels (e.g., wooden boards), because mulch fuel beds are relatively porous. This porosity allows firebrands to embed within the recipient fuel, increasing contact between the ignition source (i.e., firebrands) and the fuel [15]. In previous, Steward et al. [11] and Zipperer et al. [16] investigated the ease of ignition of different landscape mulches at different scales, but no quantitative measures on the flammability under various environmental conditions were discussed. Rogstad et al. [10] found that a single lit cigarette could not ignite any types of mulch, while Steward et al. [11] achieved ignition using three lit filter cigarettes, attributed to the increased heating area and intensity. Manzello et al. [17] found that the ignition propensity of three types of mulch increased with the size of the deposited firebrand, indicating the critical role of contact between firebrands and mulch beds [13]. Manzello et al. [18,19] further highlighted that the ease of ignition increased with the number of firebrands, further motivating the need to study the accumulation of brands, rather than just an individual particle.

During WUI fires, firebrands tend to accumulate in piles on top of solid fuels [15,20]. The anticipated heating process induced by a firebrand pile is expected to differ from that caused by a single firebrand. This discrepancy is attributed to the interactions among individual firebrands within the pile, allowing for a reheating process [20,21]. Reheating occurs when the firebrand pile shifts, enabling higher-temperature firebrands to transfer heat to lower-temperature ones [15]. This process elevates the temperature of the inactive brands, promoting a more robust smoldering reaction [15]. Both the interaction among individual firebrands within the pile and the contact between firebrands and the recipient fuel are expected to alter the heat transfer mechanisms governing the ignition process of a solid fuel. However, there has been limited prior research on the ignition of vegetative fuels by accumulations of firebrands.

When lofted firebrands land on a recipient mulch bed, the mulch may first be heated and dried before beginning to decompose and smolder [22,23]. In general, smoldering can be initiated by a weak heat source, providing a shortcut to flaming through smoldering-to-flaming (StF) transition [24–28]. The StF transition is a stochastic process where smoldering reactions provide the heat necessary to pyrolyze virgin fuel, and meanwhile act as a pilot to ignite flammable gaseous mixtures [29,30]. With a sufficient oxygen supply, smoldering mulch beds may transition to flaming and subsequently ignite nearby features such as fencing assemblies or siding materials through direct flame contact and radiant heat exposure [6,14]. However, limited research has quantified the thresholds of ignition and StF transition, and their sensitivity to firebrand loading.

In this work, spotting smoldering ignition of four mulch samples by firebrand piles and their subsequent transition to flaming were investigated in a wind tunnel with an external wind speed of up to 1.4 m/s. First, the heat flux and heating duration provided by the firebrand pile to an inert surface were quantified. Afterwards, the thresholds of smoldering ignition and transition to flaming were determined as a function of external wind speeds and the initial mass of firebrand piles. A simplified heat transfer model was proposed to explain the influence of firebrand configuration on the ignition boundaries of mulch samples, and the effect of mulch particle size was also discussed.

2. Experimental details

2.1. Materials

Four different kinds of non-composted mulch, namely black mulch (BM), forest floor (FF), redwood (RW), and fir bark (FB), were selected in this study (Fig. 1(a)). These products were directly sourced from commercial suppliers in Marin County, California, USA without further processing (except drying), and their size distributions can be found in Appendix (Fig. A1). Before the tests, all mulch samples were dried in an oven at 90 °C for 48 h. The volatile content of the mulch sample was measured as the weight percent of gas (emissions) from the mulch sample during heating from 25 °C to 800 °C at a rate of 30 °C/min in an oxygen-free environment using a PerkinElmer STA 6000 Simultaneous Thermal Analyzer. A C/H/N elemental analysis was also performed using a Thermo Fisher Flash*Smart* Elemental analyzer. The physical properties of the mulch samples are summarized in Table 1. To investigate the effect of particle size (D), FBs with two different particle size distributions were selected. The particle sizes of fir bark A are mainly distributed between 0.6 and 1.9 cm. For fir bark B, the sizes of all particles are smaller than 1.3 cm, and more than half of the particles are smaller than 0.6 cm. The porosity of the fuel bed can be calculated as $\psi = 1 - \rho_b/\rho_s$, where ρ_b is the bulk density, and ρ_s is the solid density. From Table 1, as the bulk densities of fir bark A and fir bark B are very close, their porosities are also similar.

2.2. Experimental setup and test procedures

Experiments were conducted in a small-scale rectangular wind tunnel with a 55 cm (length) × 13 cm (width) × 8 cm (height) test section which can provide a uniform wind speed of up to 1.4 m/s, as shown in Fig. 1(b). The burning process inside the wind tunnel was observed and recorded through a transparent glass window on the front side of the wind tunnel. A mulch fuel bed (13 cm × 8 cm × 3 cm) was filled into a reactor made of 1-cm ceramic insulation board that was mounted horizontally along the floor of the tunnel test section [31]. To measure the critical surface temperature for self-sustaining smoldering and

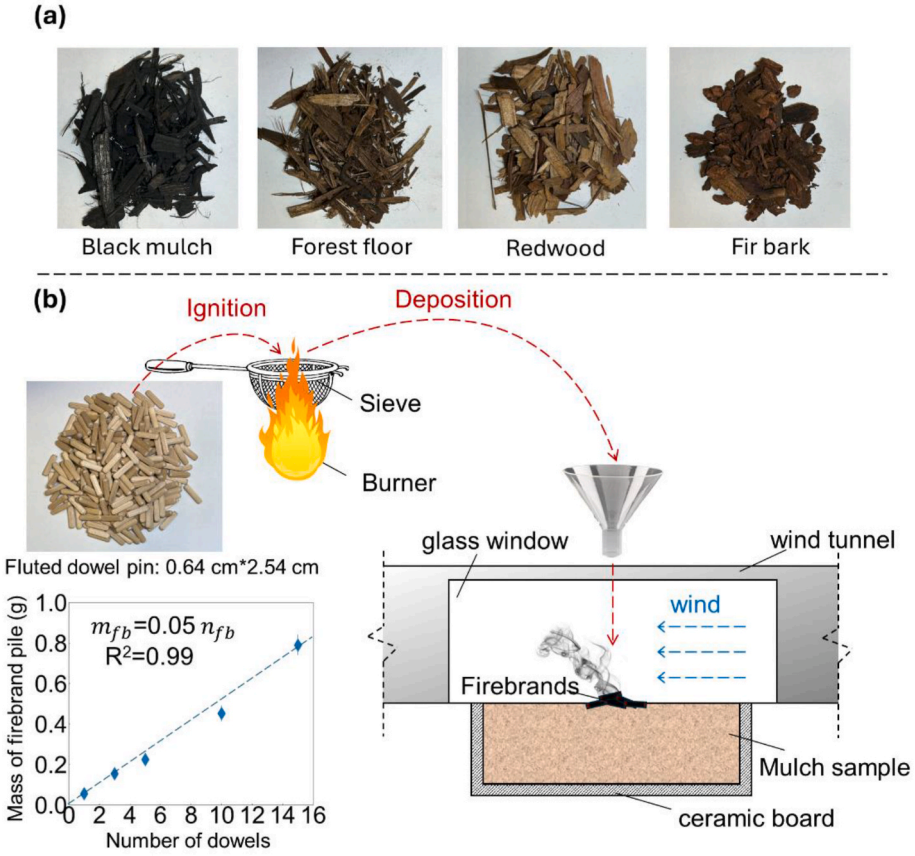

Fig. 1. (a) Photos of mulch samples tested in this work, and (b) schematic of experimental setup and procedure.

Table 1
Physical properties of the mulch.

mulch type	bulk density (kg/m^3)	volatile fraction (%)	C (%)	H (%)	N (%)
Black mulch	130	86.6	46.4	6.2	0.1
Forest floor	157	66.1	44.9	6.1	0.5
Redwood	152	85.8	47.8	6.4	0.2
Fir bark A	253	70.9	47.0	6.2	0.1
Fir bark B	247				

smoldering-to-flaming transition, an infrared camera (FLIR-64501) (25–650 °C) and color pyrometry (600–1200 °C) were used to record the top-surface temperature of mulch samples from the top with a time interval of 1 s. The IR camera came factory-calibrated and an emissivity of 0.9 was assumed for the burning mulch [32]. The color pyrometry was performed using a Sony Alpha 1 camera with a full-frame 35.9 × 24.0 mm stacked Exmor RS CMOS sensor, pixel dimensions of 8640 × 5760, and a bit depth of 16 in each color plane. The lens was a Sony FE 24–70 mm GM Full-frame G Master standard zoom lens. The color pyrometry setup was calibrated using a blackbody radiation source within the temperature range studied. More details on image capture, calibration, and processing can be found in Ref. [33].

Smoldering firebrands were generated by placing different numbers of equal mass wooden dowels (0.64 cm × 2.54 cm) in a wire mesh basket which was then set on top of a propane burner for about 10 s until a self-sustained flame fully covering the dowels was observed [34]. The burner was then extinguished and firebrands were allowed to burn freely (~10 s) until self-extinction of the flame occurred, followed by a self-sustaining smoldering process [31,35,36]. To generate different masses of firebrand piles, different numbers of dowels (i.e., 1, 3, 5, 10, 15) were used, and the masses of smoldering firebrand piles were quantified, as shown in Fig. 1(b). For example, as the number of dowels increases from 1 to 15, the mass of firebrand piles increases from 0.06 g to 0.79 g. A linear correlation between the number of dowels (n_{fb}) and the mass of the firebrand pile (m_{fb}) was also found as $m_{fb} = 0.05 n_{fb}$, with $R^2 = 0.99$.

The smoldering firebrands were deposited onto the middle of the mulch sample surface using a funnel-like apparatus with an outlet diameter of 2 cm, similar to our previous works [34,35,37]. The deposition of all brands at once may represent a greater heating load than occurs for the same mass of firebrands distributed over a range of time in a wildland fire; however, this represented a repeatable worst-case scenario [4,34,38]. Following deposition, an external wind was applied parallel to the mulch surface. Successful smoldering ignition was defined as the observation of a blackened smoldering front successfully propagating outwards from the heating region that eventually burned out the mulch sample (with mass loss >80 %) [31]. If smoldering ignition was not achieved, a new test with a fresh sample was performed but a higher airflow or a larger mass of firebrand pile was applied. Afterwards, the airflow speed and the mass of firebrands were further adjusted to quantify the boundary of the StF transition. For each scenario, at least three repeated tests were conducted, and good experimental repeatability was found. During the tests, the ambient temperature was around 25 °C and the relative humidity was around 50 %.

2.3. Characteristics of the firebrand piles

To quantify the heat flux from a burning firebrand pile, the mulch fuel bed was first replaced by a sheet of 1.27 cm thick ceramic fiber insulation board. A calibrated water-cooled total heat flux gauge (WC-HFG, 1.27 cm diameter Medthern Schmidt-Boelter model GTW-7-32-485A) was inserted at the center of the board to measure the heat flux

from the smoldering pile, following a similar procedure introduced in Ref. [37]. Note that the heat flux from a firebrand pile to a recipient fuel is a complex process [39], but the use of an inert surface simplifies this somewhat by removing interactions between the firebrand pile and recipient fuel [37]. However, if the firebrand piles directly land on a porous media with an uneven surface, a higher heat flux from a smoldering pile may be received by particles in the substrate under the same conditions because of improved contact and re-radiation between the hot particles [34]. This is somewhat different from what may happen on a solid substrate, where cooling by the large thermal mass (i.e., heat capacity) of the substrate may slightly decrease heating vs. measurements taken over inert samples [21,40].

Fig. 2(a–b) shows some typical examples of time-resolved heat fluxes measured by the heat flux gauge. When the firebrand pile was first deposited, the heat flux significantly increased to its peak value. The initial peak occurs early in the test time and was difficult to see, therefore we have included an inset in the Appendix to better visualize these heat fluxes. These peak heat fluxes tended to occur immediately upon deposition and were short-lived, combining both conduction and radiation until the brands quickly cooled upon contact with the heat flux gauge [20]. Afterwards, it decreased and then remained relatively stable at a constant value before gradually decreasing to zero due to consumption of fuel and cooling induced by both exterior wind and the sensor itself.

Fig. 2(c) summarizes the peak heat fluxes recorded from different firebrand piles under external winds. First, the peak heat flux was found to increase as the mass of the firebrand pile increased, due to a larger mass of burning brands and improved re-radiation between the hot particles [37]. On the other hand, as the external wind speed initially increased from 0 to 0.91 m/s, the peak heat flux first increased because of the improved oxygen supply [41], regardless of the initial mass of the firebrand piles. However, as the wind speed further increased, the peak heat flux started to decrease because of the increasingly dominant role of convective cooling [42]. Fig. 2(d) further summarizes the heating duration of firebrand piles, and as expected, it increased as the mass of the firebrand pile increased but decreased as the wind speed increased. Note that the surface area of the mulch sample directly covered by the firebrand pile generally increased as the mass of the firebrand pile increased, leading to a larger heating area.

3. Results and discussion

3.1. Fire phenomena of mulch

Fig. 3 shows examples of three representative paths a firebrand pile deposited on RW samples may take depending on the applied wind speed, where the initial mass of the firebrand pile was 0.23 g (see Videos S1-3). Once the firebrand pile landed on the mulch sample, a strong glowing process could be observed, because of the improved oxygen supply driven by the external wind. Afterwards, some smoke was released from the surface of the mulch sample directly covered by the firebrand pile, indicating initiation of pyrolysis and/or smoldering. After some time, an ash layer formed over the exterior surface of the firebrand and then gradually expanded towards its interior, which resulted in reduced heating to the mulch sample (see Fig. 2(a-b)).

When the wind speed was 0.76 m/s (Fig. 3(a)), as the firebrand pile gradually burned out (i.e., the heating from the firebrand pile gradually decreased to zero), the smoke intensity gradually decreased. Eventually, no smoke was released from the mulch sample and only a small portion of the surface layer covered by the firebrand pile turned black or charred. In other words, the mulch sample was not successfully ignited under this experimental condition.

When the wind speed was increased to 0.91 m/s (Fig. 3(b)), the area directly exposed to the firebrand pile also turned black (i.e., charred) first. However, as the firebrand pile burned out, the smoke intensity did not decrease; instead, the charred area gradually expanded outwards. Therefore, the mulch sample was successfully ignited by the firebrand pile and a self-sustaining smoldering front was achieved under these conditions. Eventually, the mulch sample completely burned out and turned into ash.

Further increasing the wind speed to 1.05 m/s (Fig. 3(c)), a smoldering ignition process similar to the 0.91 m/s condition was first observed. However, more glowing spots were observed during the burning process on the edges of the mulch, after which a sudden

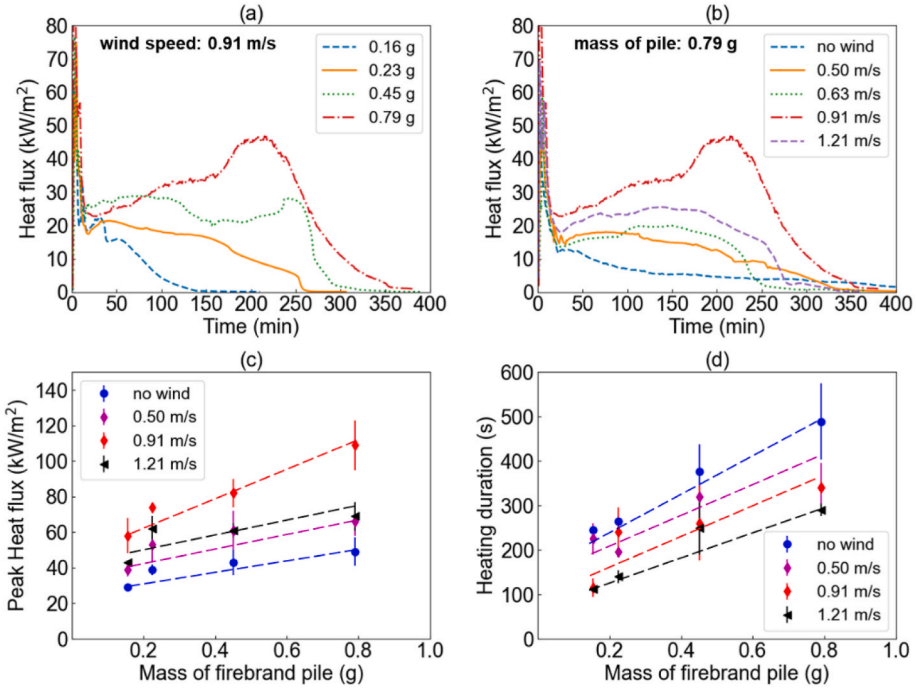

Fig. 2. (a–b) Examples of time-resolved heat fluxes of firebrand piles under external winds, and summaries of (c) peak heat fluxes and (d) heating durations where the dashed lines are linear least-squares fits to show the trends.

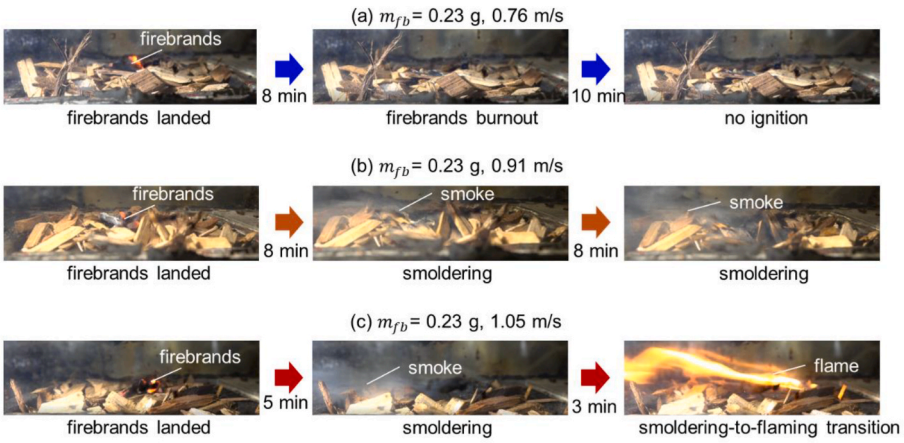

Fig. 3. Snapshots of phenomena of RW mulches heated by a firebrand pile with a mass of 0.23 g under different wind speeds.

smoldering-to-flaming transition was achieved. After burning for around 3 min, the flame self-extinguished, with the remaining mulch residue continuing to smolder until it completely burned out and turned into ash. Therefore, in real fire scenarios, the mulch around residential structures and community parks may first be ignited in a smoldering mode and later transition into a flaming fire under specific conditions, leading to a greater threat because of the sudden increase in fire spread rate, intensity and hazard [25].

3.2. Thresholds of smoldering ignition

Fig. 4 summarizes the limiting conditions of smoldering ignition of mulch and its transition to flaming under external winds, where blue crosses (×) represent no ignition, orange circles (●) represent successful smoldering ignition, and red diamonds (◆) represent smoldering ignition with subsequent transition to flaming. As shown in Fig. 4, there was a minimum mass of the firebrand pile below which the mulch sample could not be ignited, regardless of the wind speed [4]. Afterwards, the required minimum wind speed to trigger a self-sustaining smoldering reaction decreased as the mass of the firebrand pile increased. For example, for FF (Fig. 4(a)), as the mass of the firebrand pile increased from around 0.16 g to 0.48 g, the minimum wind speed decreased from around 0.85 m/s to 0.12 m/s. By gradually increasing the mass of the firebrand pile, eventually, the firebrand pile was large enough to ignite mulch without wind.

To better understand the relationship between the mass of the firebrand pile and the minimum wind speed to trigger smoldering ignition, a simplified and approximate energy conservation equation was applied [22] (see Fig. 5), where the minimum smoldering ignition energy (E_{min}) needed to not only heat the fuel up to its smoldering ignition temperature (T_{sm}), but also to overcome the conductive heat loss to the surrounding fuel ($\dot{q}''_{cond}$) and ambient heat losses ($\dot{q}''_{\infty}$) including convective and radiative heat loss as

$$E_{min} = \rho c \pi r^2 \delta (T_{sm} - T_{\infty}) + \dot{q}''_{cond}\left(2\pi r\delta + \pi r^2\right)t + \dot{q}''_{\infty}\pi r^2 t \quad (1)$$

where ρ is the bulk density of the mulch sample, r is the radius of the area covered by the firebrand pile, δ is the thermal penetration depth, c is the

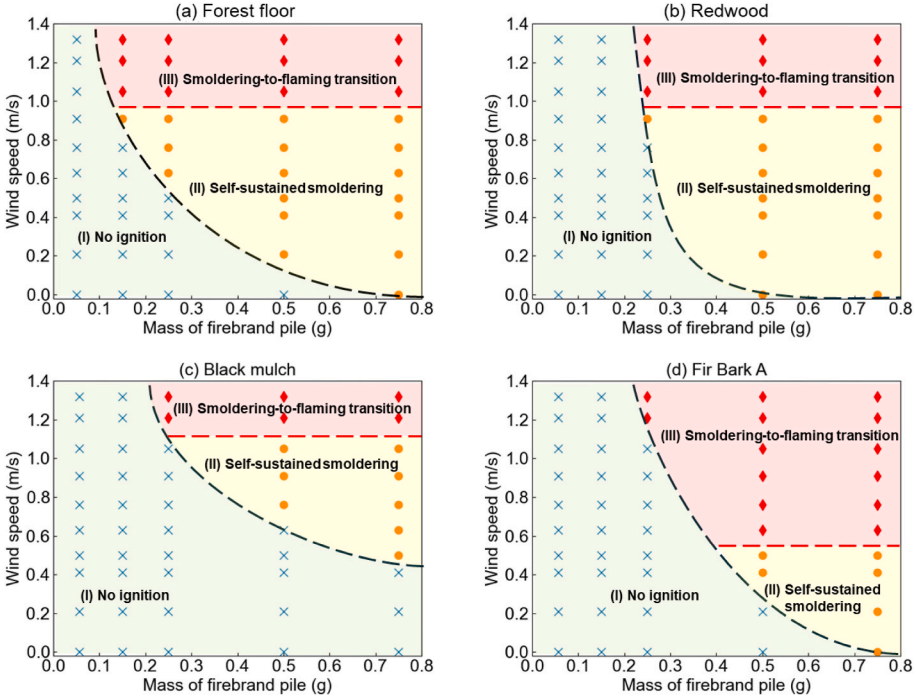

Fig. 4. Limiting conditions of smoldering ignition and its transition to flaming of different mulch samples, each marker represents at least three repeating tests.

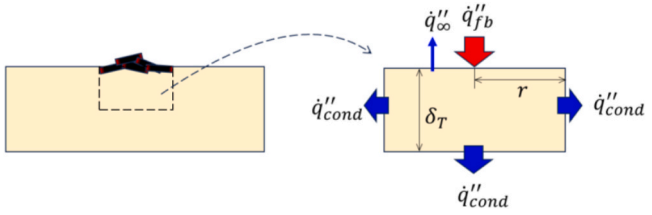

Fig. 5. Schematic of energy balance of smoldering ignition of the mulch sample by a firebrand pile.

specific heat capacity, T_∞ is the initial temperature, and t is the heating duration. Then, the required minimum ignition energy per unit area (E''_{min}) becomes

$$E''_{min} = \dot{q}''_{fb,min} t = \rho\delta c(T_{sm} - T_\infty) + \dot{q}''_{cond} t\left(\frac{2\delta}{r} + 1\right) + \dot{q}''_{\infty} t \tag{2}$$

where $\dot{q}''_{fb,min}$ is the minimum heat flux from the firebrand pile to ignite the mulch sample. By further rearranging Eq. (2), we obtain

$$\dot{q}''_{fb,min} = \frac{\rho\delta c}{t}(T_{sm} - T_\infty) + \dot{q}''_{cond}\left(\frac{2\delta_T}{r} + 1\right) + \dot{q}''_{\infty} \tag{3}$$

To achieve ignition, the heat from the firebrand pile to the mulch sample ($\dot{q}''_{fb}$) should be larger than the minimum value ($\dot{q}''_{fb,min}$) as $\dot{q}''_{fb} \geq \dot{q}''_{fb,min}$, and it could be further described as

$$\dot{q}''_{fb} = \alpha\dot{m}''_{fb}\Delta H_{sm} = \alpha\frac{\dot{m}''_{ox}}{\gamma}\Delta H_{sm} = \alpha\frac{\rho_a Y_{ox} v}{\gamma}\Delta H_{sm} \propto v \tag{4}$$

where α is the ratio of heat transferred from the firebrand pile to the mulch sample, $\dot{m}''_{fb}$ is the burning rate per unit area of the firebrand pile, ΔH_{sm} is the heat of smoldering combustion, $\dot{m}''_{ox}$ is the rate of oxygen supply, γ is the stoichiometric factor, ρ_a is the density of air, Y_{ox} is the mass fraction of oxygen in the air, v is the wind speed.

On one hand, as shown in Fig. 2, the intensity of heating from the firebrand pile to the mulch increased as the mass of the firebrand pile increased. Therefore, for a larger mass of the firebrand pile, to achieve $\dot{q}''_{fb} \geq \dot{q}''_{fb,min}$, only a smaller wind speed was required to accelerate the smoldering reaction and generate enough heat to ignite the mulch, agreeing well with the experimental observations shown in Fig. 4. On the other hand, as the heating area (or r) increased with the mass of the firebrand pile, from Eq. (3), a smaller $\dot{q}''_{fb,min}$ was required to trigger ignition when r was increased. This was consistent with our previous findings, where the critical irradiation to trigger smoldering ignition decreased as the heating area increased [22]. Therefore, only a smaller wind speed was required to intensify the reaction of a larger firebrand pile with a larger heating area to achieve $\dot{q}''_{fb} \geq \dot{q}''_{fb,min}$, which also agreed with the trend in Fig. 4.

Furthermore, from Fig. 2 and Eq. (3), as the mass of the firebrand pile decreased, $\dot{q}''_{fb}$ would decrease while the $\dot{q}''_{fb,min}$ would increase (due to a smaller heating area (i.e., r)). Eventually, there was a minimum mass of firebrand pile where the $\dot{q}''_{fb}$ could no longer be higher than $\dot{q}''_{fb,min}$, that is, no ignition could be achieved. This further demonstrated the existence of the minimum mass of the firebrand pile to trigger ignition shown in Fig. 4.

3.3. Limits of smoldering-to-flaming transition

Once a mulch sample was ignited into a smoldering mode by a firebrand pile, if the wind speed was high enough, smoldering could suddenly transition to flaming. Fig. 4 also summarizes these smoldering-to-flaming transition thresholds, and the required wind speed to trigger StF transition was insensitive to the initial mass of the firebrand pile but varied with the type of mulch. For example, for FF shown in Fig. 4(a), the smoldering could abruptly transition to flaming when the wind speed was larger than 0.98 m/s, regardless of the initial mass of the firebrand pile.

Fig. 6 summarizes the critical surface temperature (the hottest zone) measured by an IR camera, two-color pyrometry, or both, at the moment of smoldering-to-flaming transition and the minimum temperature for self-sustaining smoldering measured during experiments. First, the minimum temperature to support a self-sustaining smoldering fire was around 350 °C, agreeing well with other wooden materials reported in the literature [24]. More importantly, the critical temperature for smoldering-to-flaming transition was found to be about 850 °C, which was consistent with the characteristic temperature of the StF transition previously found for wood blocks [29], biomass rods [43] and cellulose layers [44]. To achieve smoldering-to-flaming transition, glowing particles were required to pilot the flammable mixture of pyrolysate and air [29,30]. Therefore, a larger wind speed was required to improve the oxygen supply, leading to vigorous smoldering with a high enough temperature to trigger smoldering-to-flaming transition.

Note that when the mass of the firebrand pile was relatively small (but larger than the minimum mass to trigger smoldering ignition), a higher external wind speed was required to achieve smoldering ignition, and eventually the boundaries of smoldering ignition and smoldering-to-flaming transition merged. Under this circumstance, smoldering ignition could always be achieved first followed by transition to flaming. For example, for fir bark A (Fig. 4(d)), when the mass of the firebrand pile was smaller than 0.41 g but larger than 0.21 g, the boundaries of smoldering ignition and smoldering-to-flaming transition merged into one threshold, above which smoldering could first ignite and subsequently transition to flaming.

3.4. Effect of particle size in the mulch fuel bed

Particle sizes in porous fuel beds are one of the leading factors affecting the ease of smoldering ignition and rate of smoldering propagation [45–50]. To explore the effect of mulch particle size on spotting ignition, Fig. 7 compares the limiting conditions of smoldering ignition of fir bark A (more large particles) and fir bark B (more small particles). For fir bark A with more larger particles, a smaller minimum mass of the firebrand pile was required to achieve ignition. Meanwhile, given a fixed mass of the firebrand pile, as the mulch particle size decreased, the minimum wind speed to trigger smoldering ignition also increased.

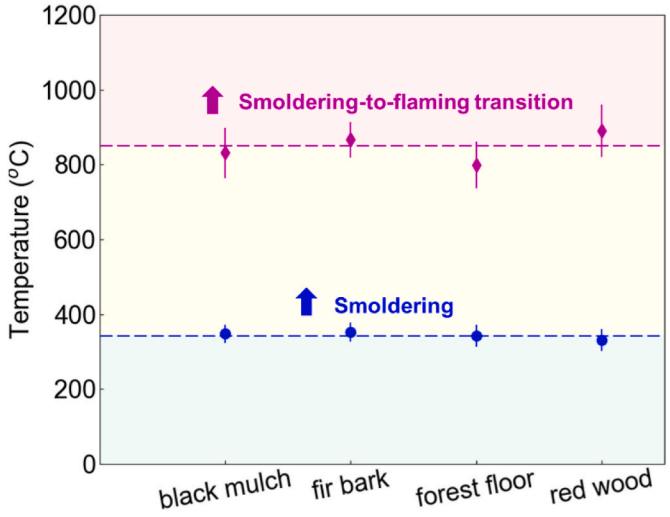

Fig. 6. Critical surface temperature measured for self-sustaining smoldering and smoldering-to-flaming transition of different mulch samples.

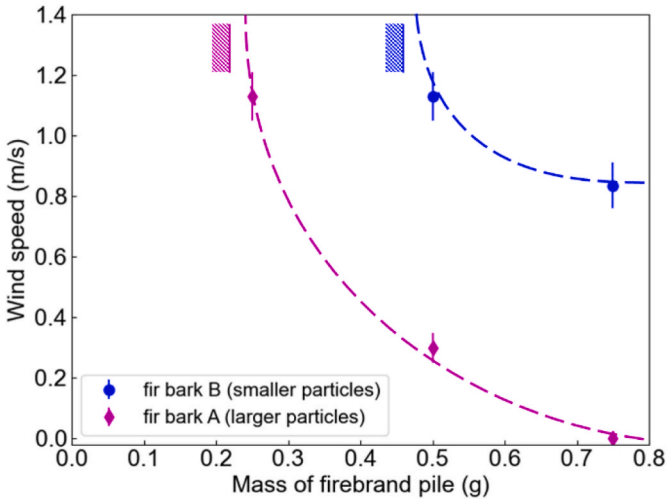

Fig. 7. Comparison of limiting conditions of smoldering ignition of fir bark mulches with different particle sizes by firebrand piles under external winds.

Furthermore, no smoldering-to-flaming transition was observed for fir bark B in the test range. Therefore, mulch with relatively larger particles may be more easily ignited by firebrand piles and subsequently transition to flaming, at least for the present experimental conditions.

On one hand, when the fuel particle was larger, the pores or channels between particles were larger, thus the oxygen can more easily diffuse through the porous media to sustain a smoldering fire and subsequent smoldering-to-flaming transition. On the other hand, for a fuel bed with a larger particle size, the top surface of the fuel bed was relatively uneven, and the shallow depressions on the fuel bed surface may be the most susceptible to firebrand accumulation and ignition [4]. These shallow depressions were similar to a crevice geometry (a common feature of some structure features at the wildland-urban interface) receiving a higher heat flux from a smoldering firebrand pile than a flat plate under the same condition due to re-radiation between the hot particles [34], which increased the likelihood of ignition.

4. Conclusions

In this work, well-controlled experiments were conducted to investigate the limiting conditions of smoldering ignition of mulch by glowing firebrand piles and the subsequent smoldering-to-flaming transition under external winds. We found that the peak heat flux, heating duration and heating area all increased with the mass of the firebrand pile within the test range. However, as the wind speed increased, the peak heat flux first increased due to an increased oxygen supply, but then decreased due to competition with increased convective cooling.

For a larger firebrand pile, no external wind was required to trigger smoldering ignition of mulch. However, as the mass of the firebrand pile decreased, a larger wind speed was required to intensify the reaction of the brands and thus heat the mulch samples sufficiently to achieve smoldering ignition. Eventually, there was a minimum mass of firebrand pile to trigger ignition. A simplified heat transfer analysis was proposed which explained the phenomenological relationship between wind speed and the mass of firebrand piles by including the heating area and two-dimensional cooling effects.

Smoldering-to-flaming transition was observed when the wind speed was larger than a critical value which was insensitive to the mass of the firebrand pile but varied with the mulch fuel types. A critical smoldering-to-flaming temperature of around 850 °C was found. Finally, the mulch sample with a larger particle size can be more easily ignited by a firebrand pile in a smoldering state and subsequently transitioned to flaming. This work provided necessary information about the ignition and smoldering-to-flaming transition for mulch, which was an important step towards understanding realistic fire scenarios at the wildland-urban interface. Future experimental and numerical work is still needed to better understand the coupling between gas- and solid-phase processes leading to the smoldering-to-flaming transition.

Availability of data and materials

The datasets generated during and/or analysed during the current study are available from the corresponding author on reasonable request.

CRediT authorship contribution statement

Shaorun Lin: Writing – original draft, Resources, Methodology, Investigation, Formal analysis, Data curation. **Chengze Li:** Investigation. **Mackenzie Conkling:** Investigation. **Xinyan Huang:** Writing – review & editing, Resources, Methodology, Formal analysis. **Stephen L. Quarles:** Writing – review & editing, Methodology, Formal analysis, Conceptualization. **Michael J. Gollner:** Writing – review & editing, Supervision, Resources, Project administration, Methodology, Funding acquisition, Formal analysis, Conceptualization.

Declaration of competing interest

The authors declare that they have no known competing financial interests or personal relationships that could have appeared to influence the work reported in this paper.

Data availability

Data will be made available on request.

Acknowledgements

This work was funded by the National Institute of Standards and Technology (NIST) Fire Research Grant 60NANB23D220, the Insurance Institute for Business & Home Safety (IBHS), the Marin Wildfire Prevention Authority, the UL Fire Safety Research Institute, and the Powley Fund at the University of California, Berkeley. The authors would like to thank Wallis Lee Robinson and Yana Valachovic (University of California Cooperative Extension, Humboldt-Del Norte Counties) and Professor Emeritus Susan Marshall (Cal Poly Humboldt, Department of Forestry, Fire and Range Management) for their help in the particle size determination.

Appendix B. Supplementary data

Supplementary data related to this article can be found at https://doi.org/10.1016/j.firesaf.2024.104226.

Appendix

Figure A1 shows particle size distributions of the mulch samples determined by passing the mulch through a series of sieves with gradually

reducing hole sizes.

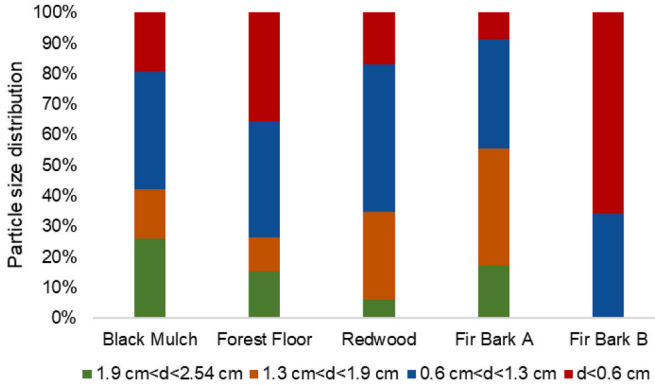

Fig. A1. Particle size distributions based on mass of mulch samples.

Figure A2 shows an inset of Fig. 2 a and b so that the initial peak in heat flux occurring when smoldering particles are deposited are better visible.

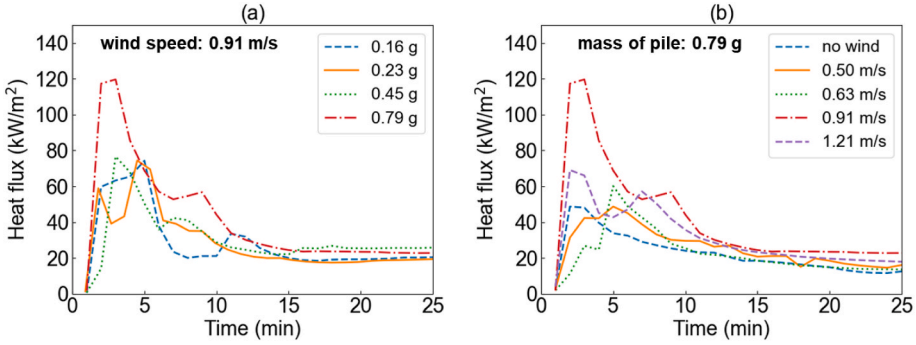

Fig. A2. Insets of Fig. 2(a–b) to better illustrate the early-time initial peaks of heat flux curves.

References

[1] S.L. Manzello, S. Suzuki, M.J. Gollner, A.C. Fernandez-Pello, Role of firebrand combustion in large outdoor fire spread, Prog. Energy Combust. Sci. 76 (2020) 100801, https://doi.org/10.1016/j.pecs.2019.100801.

[2] R. Wadhwani, C. Sullivan, A. Wickramasinghe, M. Kyng, N. Khan, K. Moinuddin, A review of firebrand studies on generation and transport, Fire Saf. J. 134 (2022) 103674, https://doi.org/10.1016/j.firesaf.2022.103674.

[3] A.C. Fernandez-Pello, Wildland fire spot ignition by sparks and firebrands, Fire Saf. J. 91 (2017) 2–10, https://doi.org/10.1016/j.firesaf.2017.04.040.

[4] S.L. Manzello, S. Suzuki, M.J. Gollner, A.C. Fernandez-Pello, Role of firebrand combustion in large outdoor fire spread, Prog. Energy Combust. Sci. 76 (2020) 100801, https://doi.org/10.1016/j.pecs.2019.100801.

[5] S. Lin, T. Zhang, X. Huang, M.J. Gollner, The initiation of smoldering Peat fire by a glowing firebrand, Int. J. Wildland Fire 33 (2024), https://doi.org/10.1071/WF23116.

[6] R.S.P. Hakes, S.E. Caton, D.J. Gorham, M.J. Gollner, A review of pathways for building fire spread in the wildland urban interface Part II: Response of components and systems and mitigation strategies in the United States, Fire Technol. 53 (2017) 475–515, https://doi.org/10.1007/s10694-016-0601-7.

[7] S.E. Caton, R.S.P. Hakes, D.J. Gorham, A. Zhou, M.J. Gollner, Review of pathways for building fire spread in the wildland urban interface Part I: exposure conditions, Fire Technol. 53 (2017) 429–473, https://doi.org/10.1007/s10694-016-0589-z.

[8] Cal Fire, Camp Fire, 2020 n.d. https://www.fire.ca.gov/incidents/2018/11/8/camp-fire/.

[9] A. Maranghides, E. Link, W. Ruddy, Mell, S. Hawks, M. Wilson, W. Brewer, C. Brown, B. Vihnaneck, W.D. Walton, A Case Study of the Camp Fire – Fire Progression Timeline, 2021, https://doi.org/10.6028/NIST.TN.2135. Gaithersburg, MD.

[10] A. Orgstad, T. Degomez, C. Hayes, J. Schalau, J. Kelly, Comparing the Ignitability of Mulch Materials for a Firewise landsCape, The University of Arizona Cooperative Extension, 2011, pp. 1–5.

[11] L.G. Steward, T.D. Sydnor, B. Bishop, The ease ofignition of 13 landscape mulches, J. Arboric. 29 (2003) 317–321.

[12] S.L. Manzello, S. Suzuki, D. Nii, Full-scale experimental investigation to quantify building component ignition vulnerability from mulch beds attacked by firebrand showers, Fire Technol. 53 (2017) 535–551, https://doi.org/10.1007/s10694-015-0537-3.

[13] S.E. Caton, R.S.P. Hakes, D.J. Gorham, A. Zhou, M.J. Gollner, Review of pathways for building fire spread in the wildland urban interface Part I: exposure conditions, Fire Technol. 53 (2017) 429–473, https://doi.org/10.1007/s10694-016-0589-z.

[14] E.L. Johnsson, A. Maranghides, Effects of wind speed and angle on fire spread along privacy fences, National Institute of Standards & Technology (2016) 1–28.

[15] R.S.P. Hakes, H. Salehizadeh, M.J. Weston-Dawkes, M.J. Gollner, Thermal characterization of firebrand piles, Fire Saf. J. 104 (2019) 34–42, https://doi.org/10.1016/j.firesaf.2018.10.002.

[16] W. Zipperer, A. Long, B. Hinton, A. Maranghides, W. Mell, Mulch flammability, Proceedings of Emerging Issues along Urban-Rural Interfaces II: Linking Land-Use Science and Society, 2007, pp. 192–195.

[17] S.L. Manzello, T.G. Cleary, J.R. Shields, J.C. Yang, Ignition of mulch and grasses by firebrands in wildland–urban interface fires, Int. J. Wildland Fire 15 (3) (2006) 427–431, https://doi.org/10.1071/WF06031.

[18] S.L. Manzello, T.G. Cleary, J.R. Shields, J.C. Yang, On the ignition of fuel beds by firebrands, Fire Mater. 30 (2006) 77–87, https://doi.org/10.1002/fam.901.

[19] S.L. Manzello, Y. Hayashi, T. Yoneki, Y. Yamamoto, Quantifying the vulnerabilities of ceramic tile roofing assemblies to ignition during a firebrand attack, Fire Saf. J. 45 (2010) 35–43, https://doi.org/10.1016/j.firesaf.2009.09.002.

[20] Z. Tao, B. Bathras, B. Kwon, B. Biallas, M.J. Gollner, R. Yang, Effect of firebrand size and geometry on heating from a smoldering pile under wind, Fire Saf. J. 120 (2021) 103031, https://doi.org/10.1016/j.firesaf.2020.103031.

[21] J.A. De Beer, J.A. Alascio, S.I. Stoliarov, M.J. Gollner, Analysis of the thermal exposure and ignition propensity of a lignocellulosic building material subjected to a controlled deposition of glowing firebrands, Fire Saf. J. 135 (2023) 103720, https://doi.org/10.1016/j.firesaf.2022.103720.

[22] S. Wang, S. Lin, Y. Liu, X. Huang, M.J. Gollner, Smoldering ignition using a concentrated solar irradiation spot, Fire Saf. J. 129 (2022), https://doi.org/10.1016/j.firesaf.2022.103549.

[23] J.L. Urban, J. Song, S. Santamaria, C. Fernandez-pello, Ignition of a spot smolder in a moist fuel bed by a firebrand, Fire Saf. J. 108 (2019) 102833, https://doi.org/10.1016/j.firesaf.2019.102833.

[24] S. Lin, H. Yuan, X. Huang, A computational study on the quenching and near-limit propagation of smoldering combustion, Combust. Flame 238 (2022), https://doi.org/10.1016/j.combustflame.2021.111937.

[25] M.A. Santoso, E.G. Christensen, J. Yang, G. Rein, Review of the transition from smouldering to flaming combustion in wildfires, Front. Mech. Eng. 5 (2019), https://doi.org/10.3389/fmech.2019.00049.

[26] P. Garg, I. Shan, S. Lin, M. Gollner, C. Fernandez-Pello, Limiting conditions of smoldering-to-flaming transition of cellulose powder, Fire Saf. J. 141 (2023) 103936, https://doi.org/10.1016/j.firesaf.2023.103936.
[27] Y. Zhang, Y. Shu, Y. Qin, Y. Chen, X. Huang, M. Zhou, Resurfacing of underground peat fire: smoldering transition to flaming Wildfire on litter surface, Int. J. Wildland Fire (2023) 1–10, https://doi.org/10.1071/WF23128 [under Review].
[28] S. Lin, T.H. Chow, X. Huang, Smoldering propagation and blow-off on consolidated fuel under external airflow, Combust. Flame 234 (2021) 111685, https://doi.org/10.1016/j.combustflame.2021.111685.
[29] Z. Zhang, P. Ding, S. Wang, X. Huang, Smouldering-to-flaming transition on wood induced by glowing char cracks and cross wind, Fuel 352 (2023) 129091, https://doi.org/10.1016/j.fuel.2023.129091.
[30] P. Garg, I. Shan, S. Lin, M. Gollner, C. Fernandez-Pello, Limiting conditions of smoldering-to-flaming transition of cellulose powder, Fire Saf. J. 141 (2023) 103936, https://doi.org/10.1016/j.firesaf.2023.103936.
[31] S. Lin, T. Zhang, X. Huang, M.J. Gollner, The initiation of smoldering peat fire by a glowing firebrand, Int. J. Wildland Fire (2023) [under Review].
[32] M. Försth, A. Roos, Absorptivity and its dependence on heat source temperature and degree of thermal breakdown, Fire Mater. 35 (2011) 285–301, https://doi.org/10.1002/fam.1053.
[33] J.H. Baldwin, P.B. Sunderland, Ratio pyrometry of emulated firebrand streaks, Fire Saf. J. 136 (2023) 103746, https://doi.org/10.1016/j.firesaf.2023.103746.
[34] F. Richter, B. Bathras, J. Barbetta Duarte, M.J. Gollner, The propensity of wooden crevices to smoldering ignition by firebrands, Fire Technol. 58 (2022) 2167–2188, https://doi.org/10.1007/s10694-022-01247-w.
[35] H. Salehizadeh, R.S.P. Hakes, M.J. Gollner, Critical ignition conditions of wood by cylindrical firebrands, Front. Mech. Eng. 7 (2021) 1–13, https://doi.org/10.3389/fmech.2021.630324.
[36] R.S.P. Hakes, H. Salehizadeh, M.J. Weston-Dawkes, M.J. Gollner, Thermal characterization of firebrand piles, Fire Saf. J. 104 (2019) 34–42, https://doi.org/10.1016/j.firesaf.2018.10.002.
[37] Z. Tao, B. Bathras, B. Kwon, B. Biallas, M.J. Gollner, R. Yang, Effect of firebrand size and geometry on heating from a smoldering pile under wind, Fire Saf. J. 120 (2021) 103031, https://doi.org/10.1016/j.firesaf.2020.103031.
[38] S.E. Caton-Kerr, A. Tohidi, M.J. Gollner, Firebrand generation from thermally-degraded cylindrical wooden dowels, Front. Mech. Eng. 5 (2019) 1–12, https://doi.org/10.3389/fmech.2019.00032.
[39] S.L. Manzello, S. Suzuki, Exposing decking assemblies to continuous wind-driven firebrand showers, Fire Saf J (2014).
[40] J.A. De Beer, E.L. Dietz, S.I. Stoliarov, M.J. Gollner, An empirical firebrand pile heat flux model, Fire Saf. J. 141 (2023), https://doi.org/10.1016/j.firesaf.2023.104004.
[41] S. Lin, T.H. Chow, X. Huang, Smoldering propagation and blow-off on consolidated fuel under external airflow, Combust. Flame 234 (2021) 111685, https://doi.org/10.1016/j.combustflame.2021.111685.
[42] J.A. De Beer, J.A. Alascio, S.I. Stoliarov, M.J. Gollner, Analysis of the thermal exposure and ignition propensity of a lignocellulosic building material subjected to a controlled deposition of glowing firebrands, Fire Saf. J. 135 (2023) 103720, https://doi.org/10.1016/j.firesaf.2022.103720.
[43] O. Kadowaki, M. Suzuki, K. Kuwana, Y. Nakamura, G. Kushida, Limit conditions of smoldering spread in counterflow configuration: extinction and smoldering-to-flaming transition, Proceedings of the Combustion Institute 000 (2020) 1–9, https://doi.org/10.1016/j.proci.2020.05.002.
[44] J. Yang, N. Liu, H. Chen, W. Gao, Smoldering and spontaneous transition to flaming over horizontal cellulosic insulation, Proc. Combust. Inst. 37 (2019) 4073–4081, https://doi.org/10.1016/j.proci.2018.05.054.
[45] Y. Tang, W. Huang, Experimental and theoretical study of the effect of particle size on the forward propagation of smoldering coal, Fuel 312 (2022) 122903, https://doi.org/10.1016/j.fuel.2021.122903.
[46] J.J. Saastamoinen, R. Taipale, Propagation of the ignition front in beds of wood particles, Combust. Flame 123 (2000) 214–226, https://doi.org/10.1016/S0010-2180(00)00144-9.
[47] B. Li, M. Li, W. Gao, M. Bi, L. Ma, Q. Qin, C.M. Shu, Effects of particle size on the self-ignition behaviour of a coal dust layer on a hot plate, Fuel 260 (2020), https://doi.org/10.1016/j.fuel.2019.116269.
[48] A. Ronda, M. Della Zassa, A. Biasin, M.A. Martin-Lara, P. Canu, S.Z. Miry, M.A. B. Zanoni, T.L. Rashwan, J.L. Torero, J.I. Gerhard, Experimental investigation on the smouldering of pine bark, Combust. Flame 193 (2017) 81–94, https://doi.org/10.1016/j.fuel.2016.12.028.
[49] N. Fernandez-Anez, J. Garcia-Torrent, Influence of particle size and density on the hot surface ignition of solid fuel layers, Fire Technol. 55 (2019) 175–191, https://doi.org/10.1007/s10694-018-0782-3.
[50] Y. Qin, Y. Zhang, Y. Chen, S. Lin, X. Huang, Minimum oxygen supply rate for smouldering propagation : effect of fuel bulk density and particle size, Combust. Flame 261 (2024) 113292, https://doi.org/10.1016/j.combustflame.2024.113292.